

Model-Independent Comparisons of Pulsar Timings to Scalar-Tensor Gravity

M.W. Horbatsch¹ and C.P. Burgess^{1,2}

¹ *Dept. of Physics & Astronomy, McMaster University
1280 Main St. W, Hamilton, Ontario, Canada, L8S 4L8.*

² *Perimeter Institute for Theoretical Physics
31 Caroline St. N, Waterloo, Ontario, Canada N2L 2Y5.*

ABSTRACT: Observations of pulsar timing provide strong constraints on scalar-tensor theories of gravity, but these constraints are traditionally quoted as limits on the microscopic parameters (like the Brans-Dicke coupling, for example) that govern the strength of scalar-matter couplings at the particle level in particular models. Here we present fits to timing data for several pulsars directly in terms of the phenomenological couplings (masses, scalar charges, moments of inertia and so on) of the stars involved, rather than to the more microscopic parameters of a specific model. For instance, for the double pulsar PSR J0737-3039A/B we find with 95% confidence that $m_A = (1.30 \pm 0.04)m_\odot$, $m_B = (1.21 \pm 0.04)m_\odot$, while the scalar-charge to mass ratios satisfy $|a_A| < 0.25$, $|a_B| < 0.25$ and $|a_B - a_A| < 0.0022$. These constraints are independent of the details of the scalar tensor model involved, and of assumptions about the stellar equations of state. Our fits can be used to constrain a broad class of scalar tensor theories by computing the fit quantities as functions of the microscopic parameters in any particular model, reproducing in particular standard constraints when applied to Brans-Dicke and quasi-Brans-Dicke models.

KEYWORDS: General Relativity, Gravity, Gravitation, Scalar-Tensor, Tensor-Scalar, Neutron Stars, Pulsars, Binary Pulsars, Double Pulsar.

Contents

1. Introduction	1
1.1 The classic constraints	1
1.2 A more model-independent approach	3
2. Formalism	4
2.1 Keplerian and Post-Keplerian Parameters	5
2.2 PK Parameters in Scalar-Tensor Gravity	6
3. Constraints	9
3.1 The double pulsar: PSR J0737-3039A/B	10
3.2 Pulsar PSR B1534+12	11
4. Conclusions	11

1. Introduction

Although General Relativity (GR) has many applications in astrophysics and cosmology, incomplete knowledge about the gravitating bodies involved prevents using most of these as tests of the theory itself for the vast majority of systems outside of the solar system. Binary pulsars provide the rare exception to this rule, due to the great precision with which timing measurements allow the properties of their orbits to be inferred [1, 2]. These orbital properties are parameterized by the inferred values of the Keplerian parameters (like semi-major axis, a , and eccentricity, e) that define the characteristics of the Newtonian orbit of the pulsar and its partner, together with its orientation in space. They are also parameterized by a suite of post-Keplerian (PK) parameters that describe observable slow, secular orbital changes over time, as well as relativistic time delays in the propagation of radio signals emitted by the pulsar.

1.1 The classic constraints

GR predicts the values for these post-Keplerian parameters in terms of the underlying Keplerian parameters and the masses $m_{A,B}$ of the two orbiting bodies. To test these predictions, bands are drawn in the $m_A - m_B$ plane, of the form

$$\xi^{\text{th}}(m_A, m_B) = \xi^{\text{obs}} \pm \Delta, \tag{1.1}$$

where ξ^{th} denotes the theoretically predicted value of a PK parameter, ξ^{obs} denotes its observed value and Δ denotes the observational error. The validity of GR requires all such bands to have non-empty intersection, providing a substantive test provided at least three

PK parameters can be measured. The area of mutual overlap then gives the GR-inferred masses of the stars, to within some tolerance.

Thus far, general relativity has passed these stringent tests, using a number of binary pulsars. For two of these — PSR B1534+12 [3, 4] and the double binary, PSR J0737-3039A/B [5, 6] — the tests are particularly redundant since it is possible to infer observational values for five independent PK parameters. It is also possible to infer the spin-orbit precession frequency [4, 6], which can be considered as a sixth PK parameter. Moreover, for the double binary, PSR J0737-3039A/B, both stars are pulsars, and a measurement of the ratio of the semi-major axes yields another constraint on the masses. The masses are constrained quite accurately

$$m_A = 1.3381(7) m_\odot \quad \text{and} \quad m_B = 1.2489(7) m_\odot \quad (\text{GR}). \quad (1.2)$$

The success of GR in describing pulsar orbits also constrains alternative theories of gravity; requiring their predictions to agree with GR to within present errors. Prominent among these alternatives are scalar-tensor theories [7], for which long-range gravitational forces are mediated by both the metric, $g_{\mu\nu}$, and a very light scalar, ϕ , described by the action

$$S = - \int d^4x \sqrt{-g} \left[\frac{1}{2\kappa^2} g^{\mu\nu} (R_{\mu\nu} + \partial_\mu \phi \partial_\nu \phi) \right] + S_m. \quad (1.3)$$

Here $\kappa^2 = 8\pi G = M_p^{-2}$ denotes the gravitational coupling, while $S_m = S_m[g_{\mu\nu}, \phi, \Psi_i]$ denotes the matter action, and controls how ϕ and $g_{\mu\nu}$ couple to the various other ‘matter’ fields, Ψ_i , which we take in what follows to have the form

$$S_m = S_m[A^2(\phi) g_{\mu\nu}, \Psi_i]. \quad (1.4)$$

This form of coupling has several motivations. First, it is favored by strong observational constraints [8] on violations of the weak equivalence principle, which are evaded by actions of the form of eq. (1.4). Second, it is also the kind of theory that actually describes the low-energy limit of certain types of extra-dimensional theories [9].

The predictions of theories of this type have been compared in detail with binary pulsar data [10, 11], with the coupling function assumed to have the particular *quasi-Brans Dicke* form,¹

$$A(\phi) = \exp \left[a_s \phi + \frac{b_s}{2} \phi^2 \right], \quad (1.5)$$

for which the effective coupling of scalars to matter turns out to have the strength

$$a(\phi) := \frac{d \ln A}{d\phi} = a_s + b_s \phi. \quad (1.6)$$

This form is motivated by the idea that the field ϕ does not vary appreciably in any particular system of interest, and so $a(\phi)$ is approximately constant.

Comparison with solar system and pulsar data is found to constrain the microscopic couplings for this theory, a_s and b_s , to be consistent with zero, with a_s strongly constrained

¹Brans Dicke theory corresponds to the specific choice $b_s = 0$.

from solar-system data and b_s restricted by pulsars. The constraints on these microscopic couplings are usually presented as an exclusion plot in the b_s - a_s plane, and in particular it was found that [10, 11]:

$$b_s \gtrsim -4.5, \quad |a_s + b_s \phi_\infty^{SS}| < 3.4 \cdot 10^{-3}, \quad (1.7)$$

where ϕ_∞^{SS} is the value of the scalar field asymptotically far away from the solar system, which is conventionally taken to be zero.

1.2 A more model-independent approach

There are two related drawbacks to traditional comparisons between scalar-tensor theory and observations. First, because limits like eq. (1.7) are quoted directly for the microscopic couplings, a_s and b_s , a completely new analysis is required for each new assumed functional form for the coupling function $A(\phi)$. Second, as discussed below (and remarked on by the original authors), these bounds are subject to uncertainties that are hard to quantify, due to limits of our understanding of the nuclear equation of state that applies within the pulsars.

In the present paper we take a complementary approach to confronting pulsar observations with scalar-tensor models, based on the observation that the scalar-tensor predictions for the PK parameters depend only on a relatively small number of macroscopic quantities that characterize how the two stars couple to the scalar field. There turn out to be seven of these, (defined in detail in section 2.2): $m_{A,B}$, $a_{A,B}$, $b_{A,B}$ and k_A . These generalize the two masses — m_A and m_B — that suffice to make predictions within General Relativity, to include four new quantities — $a_{A,B}$ and $b_{A,B}$ — that characterize the strength with which the scalar field couples to the pulsar and its orbital partner, plus one variable, k_A , related to the pulsar’s moment of inertia.

The key point is that model-dependent complications, like the detailed form of $A(\phi)$ and knowledge of the nuclear equation of state, enter only into the predictions for the quantities $m_{A,B}$, $a_{A,B}$, $b_{A,B}$ and k_A as functions of the microscopic couplings in a particular scalar-tensor theory. But these complications do *not* enter at all into the formulae that express how $m_{A,B}$ through k_A determine the observed PK parameters.

This makes it useful to phrase the confrontation between theory and experiment in two steps: first use the observations to constrain the quantities $m_{A,B}$ through k_A once and for all in a model-independent way; then compute these quantities within specific scalar-tensor models as functions of the underlying model parameters that define the function $A(\phi)$.

It is the goal of this paper to perform the first — and model-independent — one of these steps. At first sight this might seem to be impossible to do, since it appears to involve constraining more quantities than the five observable PK parameters². However, it turns out that the present data nonetheless allow useful constraints to be achieved, for two reasons. First, constraints are possible because the dependence of the PK parameters on two of the parameters, $b_{A,B}$, is very weak; thus effectively reducing the number of free variables from seven down to five.

²Since the theoretical prediction for the spin-orbit precession frequency has not yet been calculated in scalar-tensor gravity, we do not include it in the present analysis.

Second, one combination of Keplerian parameters — the ratio of projected semi-major axes of the two orbits, $R \equiv x_B/x_A$ (see section 2.1 for details of notation) — can sometimes also be measured. For instance for the double pulsar observations give $R = 1.0714(11)$. This measurement is useful because the theoretical prediction for this quantity in all Lorentz-invariant theories of gravity is $R_{\text{th}} = m_A/m_B$ and so is completely independent of the scalar couplings $a_{A,B}$ and k_A [11] (see also section 2.1). When this ratio is measurable the number of observational constraints to be satisfied rises from five to six.

In the end we find that interesting model-independent constraints on $m_{A,B}$ and $a_{A,B}$ are possible. The great virtue of these bounds is that they directly constrain the stellar parameters on which the PK parameters depend, independent of any assumptions about the function $A(\phi)$ and the nuclear equation of state.

Once the observational constraints on these quantities are known, they can be used to constrain the microscopic parameters for any choice of $A(\phi)$ or equation of state as a separate step. When we do so for the quadratic model $A(\phi) = \exp(a_s\phi + b_s\phi^2/2)$, we find agreement with earlier work, which already rules out a large part of the most interesting region (that of spontaneous scalarization [10, 11, 12]).

It might come as a surprise to the reader that this second step might depend on the details of the neutron equation of state, since it is an important feature of general relativity that predictions for the PK parameters depend only on the two masses, $m_{A,B}$, of the stars, and on none of their other properties. This happy property is called the ‘principle of effacement’ of internal structure [13], and it is this feature that allows a precise prediction of all PK parameters in GR using only the masses, without need for detailed knowledge about the star’s structure.

In scalar-tensor gravity (as in most other alternative theories of gravity) the principle of effacement does not hold. The prediction for the PK parameters actually depends in principle on all seven of the quantities which characterize the internal gravitational fields: $m_{A,B}$, $a_{A,B}$, $b_{A,B}$, k_A . For now, it is important to note that these are all a-priori independent. Once a particular equation of state is specified, then the equations of stellar structure can be solved, and on a given branch³ of stellar configurations, the quantities a , b and k for each star can be expressed in terms of its mass m and the underlying parameters — like a_s and b_s — that define the scalar-tensor model. This is the approach taken in [10, 11]. The resulting bounds are then subject to uncertainties in the equation of state, which are hard to quantify.

We thus urge observers to express their results in this more model-independent way, which potentially can then be used by theorists to constrain a great variety of specific models. Its independence of the internal structure of the objects involved also shows that some of their physical properties – like the masses $m_{A,B}$ – can be inferred quite robustly, without making assumptions about which theory of gravity actually applies in Nature.

2. Formalism

In this section we collect expressions for the Keplerian and Post-Keplerian parameters in

³In scalar-tensor theories there may be multiple branches of stellar configurations [12].

scalar-tensor theories, following the results of [2] and references therein. We do so both to establish notation and to provide context for the bounds obtained in the next section. Experts and readers in a hurry should feel free to skip this part completely.

2.1 Keplerian and Post-Keplerian Parameters

First, a reminder of how Keplerian orbits are described, followed by the post-Keplerian parameters that describe slow secular changes to the Keplerian parameters.

Orbital description

The non-relativistic gravitational two-body problem famously predicts bound orbits to be ellipses. More specifically, in the center of mass frame the relative position vector, $\vec{r} = \vec{r}_A - \vec{r}_B$, sweeps out the trajectory of an ellipse whose shape is described by two parameters: the semi-major axis \mathbf{a} , and the eccentricity e . The positions \vec{r}_A and \vec{r}_B also separately trace out ellipses, with semi-major axes satisfying $\mathbf{a}_A/\mathbf{a} = m_B/M$ and $\mathbf{a}_B/\mathbf{a} = m_A/M$, where $M = m_A + m_B$ is the system's total mass.

The time taken to traverse this orbit is given by the orbital period P_b , and is related to the semi-major axis by Newton's modification of Kepler's Third Law: $P_b = 2\pi\mathbf{a}^{3/2}(GM)^{-1/2}$. For timing measurements a reference time, T_0 , is also needed to specify the time of passage through periastron.

The orientation of the orbital ellipse with respect to a reference triad is specified by three angles. In celestial mechanics these angles are conventionally taken to be the *longitude of ascending node*, η ; the *orbital inclination*, i , of the orbit relative to the plane of the sky; and the *argument of periastron*, ω .

Standard techniques allow the positions and momenta of the two bodies to be inferred from the variables $(\mathbf{a}, e, \eta, i, \omega, T_0)$ by means of the action-angle formalism [14].

Deviations from the Newtonian two-body problem cause the shape and orientation of the Keplerian orbits to change with time. In practice this change is slow enough to be regarded as a small secular evolution in each of the Keplerian parameters. Two of these have been accurately measured for several binary pulsars: the decrease in the orbital period due to emission of gravitational radiation, \dot{P}_b ; and the precession of the orbital periastron, $\dot{\omega}$.

Pulsar timing

Pulsars emit electromagnetic signals at regular intervals that are measured on Earth by radio telescopes. The problem of relating the time of emission T_e at the pulsar to the time of arrival τ_a on Earth is usually split into two parts. The first part involves relating T_e to the time of arrival t_a at the solar-system barycenter, neglecting the time delay due to the solar gravitational field. The second part involves relating t_a to τ_a , which depends only on the motion of Earth with respect to the solar system barycenter (and is not considered here).

The solution to the first problem is the pulsar timing formula, and is conventionally written

$$Dt_a = T_e + \Delta_R + \Delta_E + \Delta_S + \mathcal{O}(1/c^4). \quad (2.1)$$

These terms have the following origin.

- The Doppler factor D describes the time dilation caused by the motion of the solar system relative to the binary pulsar.
- The term Δ_R is called the Römer time delay. It is $\mathcal{O}(1/c)$, and is due to the dependence of the light path on the position of the pulsar. The variable that sets the time scale of the Römer delay is the projection of the semi-major axis along the line of sight, measured in units of time. It is conventionally denoted $x_{A,B} \equiv \mathbf{a}_{A,B} \sin i/c$, and is called the light crossing time.
- The term Δ_E is called the Einstein time delay. It is $\mathcal{O}(1/c^2)$, and is due to the time dilation caused by the motion of the pulsar A and the gravitational field of the companion B. The variable that sets the time scale of the Einstein delay is called γ , and is given by equation (2.10), below.
- The term Δ_S is called the Shapiro time delay. It is $\mathcal{O}(1/c^3)$, and is caused by the effect of curved space on the propagation of light. It can be thought of as the first relativistic correction to Δ_R . The variable that sets the time scale of the Shapiro delay is called r (the *range* of the Shapiro delay), and is given by equation (2.11) below. It is proportional to $G_{\infty B}$, the gravitational coupling between the companion B and a photon, whereas all the other PK parameters depend on G_{AB} , the gravitational coupling between the two orbiting bodies. It is intuitively clear that the importance of the Shapiro effect depends strongly on the inclination angle of the orbit. The variable which parametrizes this dependence is called s (the *shape* of the Shapiro delay), and is given by equation (2.12).

2.2 PK Parameters in Scalar-Tensor Gravity

When solving the problem of stellar structure in scalar-tensor gravity, it is necessary to specify the boundary condition for the scalar field asymptotically far away from the star, ϕ_∞ . All of the properties of the star, such as its mass, therefore depend implicitly on ϕ_∞ . (Because these properties can be multiple-valued functions of ϕ_∞ , for some purposes it can be useful instead to follow the dependence on the value of the scalar field at the star's centre [15].)

Although the asymptotic field is simple to specify for isolated stars, it is a more complicated concept for an orbiting binary system. For isolated stars, the scalar field sourced by the star becomes small far from its position, leading to the generic weak-field large-distance form

$$\Phi_{A,B}(t, \vec{r}) = \Phi_\infty + \frac{GQ_{A,B}}{|\vec{r} - \vec{r}_{A,B}(t)|c^2} + \dots, \quad (2.2)$$

where $Q_{A,B}$ defines the scalar ‘charges’ of the two stars, and $\vec{r}_{A,B}(t)$ are their trajectories.⁴ We here make the choice that the scalar field approaches Φ_∞ asymptotically far away from both stars of the binary system. It is convenient to choose units of length so that $\Phi_\infty = 0$.

⁴Knowledge of the stellar equation of state allows $Q_{A,B}$ to be computed as functions of the corresponding mass, $m_{A,B}$, and the asymptotic value of the scalar field.

Now consider a binary system of stars A and B, and assume that the separation between the two stars is large enough to justify the near-Newtonian weak-field limit. In this regime the fields sourced by the two stars can be superposed so the total scalar field is $\Phi = \Phi_A + \Phi_B$. Consider now the region much closer to one of the two stars, and let ϕ_A and ϕ_B denote the scalar fields of each star in this ‘internal’ regime. The boundary conditions for this ‘internal’ field therefore are (approximately)

$$(\phi_A)_\infty(t) \simeq \Phi_B(t, \vec{r}_A(t)), \quad (\phi_B)_\infty(t) \simeq \Phi_A(t, \vec{r}_B(t)). \quad (2.3)$$

These expressions show that $(\phi_{A,B})_\infty$ are small whenever $Gm/rc^2 \sim (v/c)^2 \ll 1$, where r is the separation between the two stars, and v is their orbital velocity.

Now, the couplings that are relevant for computing post-Keplerian quantities govern how the mass of star A depends on the boundary condition $(\phi_A)_\infty$. For instance, expanding m_A in a power series about $(\phi_A)_\infty = 0$, defines the coefficients a_A and b_A :

$$m_A[(\phi_A)_\infty] = m_A \left[1 + a_A(\phi_A)_\infty + \frac{1}{2} (b_A + (a_A)^2) (\phi_A)_\infty^2 + \dots \right], \quad (2.4)$$

and an expansion of m_B about $(\phi_B)_\infty = 0$ similarly defines a_B and b_B . We may define the scalar coupling functions, $a_{A,B}$ and $b_{A,B}$, by

$$a_A[(\phi_A)_\infty] \equiv \frac{\partial \log m_A[(\phi_A)_\infty]}{\partial (\phi_A)_\infty} = a_A + b_A(\phi_A)_\infty + \dots, \quad (2.5)$$

$$b_A[(\phi_A)_\infty] \equiv \frac{\partial^2 \log m_A[(\phi_A)_\infty]}{\partial (\phi_A)_\infty^2} = b_A + \dots, \quad (2.6)$$

with similar definitions for $a_B[(\phi_B)_\infty]$ and $b_B[(\phi_B)_\infty]$. It is a general property of scalar-tensor systems that couplings defined in this way agree with those defined from $A(\phi)$ using eq. (1.6) in the limit of weakly coupled non-relativistic systems.

Pulsars rotate, and the frequency of pulsation is given by the rotational frequency $\Omega = J/I$, where J is the ‘spin’ angular momentum of the pulsar, and I is its moment of inertia. I can be found by solving the equations of stellar structure, and just like the mass, it depends on the boundary conditions for the scalar field:

$$I_A[(\phi_A)_\infty] = I_A [1 - k_A(\phi_A)_\infty + \dots], \quad (2.7)$$

leading us to define

$$k_A[(\phi_A)_\infty] \equiv -\frac{\partial \log I_A[(\phi_A)_\infty]}{\partial (\phi_A)_\infty} = k_A + \dots \quad (2.8)$$

The predictions for the PK parameters in Scalar-Tensor gravity turn out to be determined by the Keplerian parameters, together with the coefficients $m_{A,B}$, $a_{A,B}$, $b_{A,B}$ and k_A [11]. Explicitly,

$$\dot{\omega} = \frac{n}{1 - e^2} \left(\frac{G_{AB} M n}{c^3} \right)^{2/3} \left(\frac{3 - a_A a_B}{1 + a_A a_B} - \frac{X_A b_B a_A^2 + X_B b_A a_B^2}{2(1 + a_A a_B)^2} \right), \quad (2.9)$$

$$\gamma = \frac{eX_B}{n(1+a_Aa_B)} \left(\frac{G_{AB}Mn}{c^3} \right)^{2/3} (X_B(1+a_Aa_B) + 1 + k_Aa_B), \quad (2.10)$$

$$r = G_{\infty B}m_B/c^3, \quad (2.11)$$

$$s = \frac{nx_A}{X_B} \left(\frac{G_{AB}Mn}{c^3} \right)^{-1/3}, \quad (2.12)$$

where $G_{AB} = G(1 + a_Aa_B)$ is the total (graviton plus scalar) weak-field coupling between the two bodies, and $G_{\infty B} = G(1 + a_{\infty}^{\text{psr}}a_B)$ is the coupling between the companion B and a non-compact body in the vicinity of the binary pulsar. The quantity a_{∞}^{psr} is given by the value of the scalar-matter coupling $a(\phi)$ (defined in equation (1.6)) asymptotically far away from the binary pulsar. As before $M = m_A + m_B$ is the total mass, while $n = 2\pi/P_b$ is the orbital angular frequency and $X_{A,B} = m_{A,B}/M$.

The expression for the decay of the orbital period is similarly given by

$$\dot{P}_b = \dot{P}_b^{\text{mon}} + \dot{P}_b^{\text{dip}} + \dot{P}_b^{\text{quad}} + \dot{P}_b^{\text{kin}} + \dot{P}_b^{\text{gal}}, \quad (2.13)$$

where the different contributions are:

$$\begin{aligned} \dot{P}_b^{\text{mon}} = & -\frac{3\pi X_A X_B}{1 + a_A a_B} \left(\frac{G_{AB} M n}{c^3} \right)^{5/3} \frac{e^2(1 + e^2/4)}{(1 - e^2)^{7/2}} \times \\ & \times \left[\frac{5}{3}(a_A + a_B) - \frac{2}{3}(a_A X_A + a_B X_B) + \frac{b_A a_B + b_B a_A}{1 + a_A a_B} \right]^2, \end{aligned} \quad (2.14)$$

$$\dot{P}_b^{\text{dip}} = -\frac{2\pi X_A X_B}{1 + a_A a_B} \left(\frac{G_{AB} M n}{c^3} \right) \frac{(1 + e^2/2)}{(1 - e^2)^{5/2}} (a_A - a_B)^2, \quad (2.15)$$

$$\begin{aligned} \dot{P}_b^{\text{quad}} = & -\frac{32\pi X_A X_B}{5(1 + a_A a_B)} \left(\frac{G_{AB} M n}{c^3} \right)^{5/3} \frac{(1 + 73e^2/24 + 37e^4/96)}{(1 - e^2)^{7/2}} \times \\ & \times (6 + [a_A(1 - X_A) + a_B(1 - X_B)]^2), \end{aligned} \quad (2.16)$$

where ‘mon’, ‘dip’, and ‘quad’ denote monopole, dipole, and quadrupole radiation, respectively. In the limit of general relativity — *i.e.* when $a_{A,B} \rightarrow 0$ and $b_{A,B} \rightarrow 0$ — the monopole and dipole contributions vanish. Note that the monopole term is of order $1/c^5$, because the total scalar charge of the binary system is constant in time.

The last two terms in equation (2.13) arise due to the relative motion between the binary pulsar and the solar system [16]. The kinetic contribution to \dot{P}_b is given by

$$\dot{P}_b^{\text{kin}} = v_T^2/cd, \quad (2.17)$$

where \vec{v} is the velocity of the binary pulsar relative to the solar system, and T denotes the component transverse to the line of sight, and d is the distance between the binary pulsar and the solar system.

The galactic contribution to \dot{P}_b is given by

$$\dot{P}_b^{\text{gal}} = a_R/c, \quad (2.18)$$

where \vec{a} is the acceleration of the binary pulsar relative to the solar system, and R denotes the component along the line of sight. We have [2]

$$\vec{a} = \left[\frac{1 + a_{\infty}^{\text{gal}} a_{\text{psr}}}{1 + (a_{\infty}^{\text{gal}})^2} \right] \vec{g}_{\text{psr}} - \vec{g}_{\text{ss}}, \quad (2.19)$$

where \vec{g}_{psr} is the acceleration of the binary pulsar relative to the galactic centre, as predicted by a Newtonian galactic model, and \vec{g}_{ss} is the corresponding quantity for the solar system. The quantity a_{∞}^{gal} is the value of the scalar-matter coupling function $a(\phi)$ (defined in equation (1.6)) asymptotically far away from the galaxy, and

$$a_{\text{psr}} = X_A a_A + X_B a_B \quad (2.20)$$

is the charge-to-mass ratio of the binary pulsar system as a whole.

A simple galactic model may be used to relate a_{∞}^{gal} to a_{∞}^{psr} , and so in principle the PK parameters depend on a_{∞}^{psr} (and the galactic model) in addition to the seven quantities $m_{A,B}$, $a_{A,B}$, $b_{A,B}$ and k_A . However, it turns out in practice that the contributions of a_{∞}^{psr} are much too small to be measurable, so we henceforth set $a_{\infty}^{\text{psr}} = a_{\infty}^{\text{gal}} = 0$. This ensures that GR is recovered asymptotically far away from the binary pulsar, and asymptotically far away from the galaxy.

Note that equations (2.9)–(2.13) are invariant under

$$a_A \rightarrow -a_A, \quad a_B \rightarrow -a_B, \quad a_{\infty}^{\text{psr}} \rightarrow -a_{\infty}^{\text{psr}}, \quad a_{\infty}^{\text{gal}} \rightarrow -a_{\infty}^{\text{gal}} \quad \text{and} \quad k_A \rightarrow -k_A, \quad (2.21)$$

which corresponds to switching the sign of the scalar field.

3. Constraints

In order to find constraints on values of the parameters $m_{A,B}$, $a_{A,B}$, $b_{A,B}$ and k_A we compute the quantity

$$\chi^2(m_A, m_B, a_A, a_B, b_A, b_B, k_A) = \sum_{i=1}^N \left[\frac{\xi_i^{\text{th}}(m_A, m_B, a_A, a_B, b_A, b_B, k_A) - \xi_i^{\text{obs}}}{\Delta_i} \right]^2, \quad (3.1)$$

where ξ_i runs over as many of the quantities \dot{P}_b , $\dot{\omega}$, γ , r , s and R as are measured for the pulsar of interest, with observed value $\xi_i^{\text{obs}} \pm \Delta_i$.

In what follows we consider two pulsars, for which at least five PK parameters have been measured. For the double pulsar PSR J0737-3039, all of these quantities are measured and so $N = 6$, implying that the range $\chi^2 < 1.63$ corresponds to 95% confidence. For the binary pulsar PSR B1534+12, by contrast, R is not measured and so $N = 5$, and the range $\chi^2 < 1.14$ corresponds to 95% confidence.

For each of these pulsars we show contour plots of values of χ^2 , after marginalization over the variables that are not shown.

Symbol	Meaning	Value
x_A	Light crossing time of A	1.415032(1)s
x_B	Light crossing time of B	1.5161(16)s
e	Eccentricity	0.0877775(9)
P_b	Orbital Period	0.10225156248(5)days
ω	Argument of periastron of A	73.805(3) $^\circ$
T_0	Time at periastron of A	52870.0120589(6)MJD

Table 1: Keplerian parameters for the Double Pulsar J0737-3039.

Symbol	Meaning	Value
\dot{P}_b	Time derivative of orbital period	$-1.252(17)10^{-12}$
$\dot{\omega}$	Precession frequency of periastron	$16.89947(68)^\circ\text{yr}^{-1}$
γ	Relativistic timing parameter	0.3856(26)
r	Range of Shapiro delay	6.21(33) μs
s	Shape of Shapiro delay	0.99974(-39, +16)

Table 2: Post-Keplerian Parameters for the Double Pulsar J0737-3039. The galactic and kinetic contributions to \dot{P}_b are negligible.

3.1 The double pulsar: PSR J0737-3039A/B

The double pulsar PSRJ0737-3039A/B [5, 6] consists of two pulsars, A and B, that are bound in a relativistic orbit described by the Keplerian parameters summarized in table 1, and the Post-Keplerian parameters summarized in table 2. Pulsar A has a period of 23ms, and pulsar B has a much slower period of 2.8s. The Post-Keplerian timing parameters γ , r , s all pertain to pulsar A. The light crossing time x has been measured for both pulsars.

The plot of χ^2 in the $a_A - a_B$ plane is shown in the left panel of figure 1. This figure is symmetric under $a_{A,B} \rightarrow -a_{A,B}$, as expected from the symmetry (2.21). It shows that $|a_A| < 0.25$ and $|a_B| < 0.25$ with 95% confidence. Moreover, it shows that a_A is very close to a_B , with a precision that is more easily seen in the right panel of the same figure. The robustness of this constraint can be simply understood from equation (2.15) – if $|a_B - a_A|$ gets too large, then this equation predicts too much dipole radiation, inconsistent with observations. From the right panel we see that $|a_B - a_A| < 0.0022$ with 95% confidence.

The plot of χ^2 in the $m_A - m_B$ plane is shown in the left panel of figure 2. We find from this that $m_A = (1.30 \pm 0.04)m_\odot$ and $m_B = (1.21 \pm 0.04)m_\odot$ with 95% confidence. The masses lie very close to the line $m_A = Rm_B$, in good agreement with the general prediction. The deviation from this line is shown in more detail in the right panel of the same figure, by plotting $x_B m_B - x_A m_A$ versus m_A . The mass values inferred in GR — $m_A = 1.3381(7)m_\odot$ and $m_B = 1.2489(7)m_\odot$ — lie at the top-right of the line in the left panel of figure 2, and in the center right of the right panel of the same figure.

3.2 Pulsar PSR B1534+12

The binary pulsar PSR B1534+12 is another system where all five PK parameters have been measured [3]. The Keplerian parameters are summarized in table 3, and the Post-Keplerian parameters are summarized in table 4.

Symbol	Meaning	Value
x_A	Light crossing time of A	3.729464(2)s
e	Eccentricity	0.2736775(3)
P_b	Orbital Period	0.420737299122(10)days
ω	Argument of periastron of A	274.57679(5) $^\circ$
T_0	Time at periastron of A	50260.92493075(4)MJD

Table 3: Keplerian Parameters for PSR B1534+12.

The $a_A - a_B$ plane is shown in the left panel of figure 3. It can be seen from this figure that $|a_A| < 0.44$ and $|a_B| < 0.44$ with 95% confidence. Just like for the double pulsar, we see that a_A must be very close to a_B , and plotting this difference in the right panel of the same figure, we find that $|a_B - a_A| < 0.0035$ with 95% confidence.

The $m_A - m_B$ plane is shown in figure 4. We find from this that $m_A = (1.1 \pm 0.2)m_\odot$ and $m_B = (1.25 \pm 0.10)m_\odot$ with 95% confidence.

4. Conclusions

In summary, we have shown that the existing data for two pulsars is constraining enough to place model-independent bounds directly on the stellar parameters that control the size of post-Keplerian effects in scalar-tensor models. The virtue of these bounds is that they

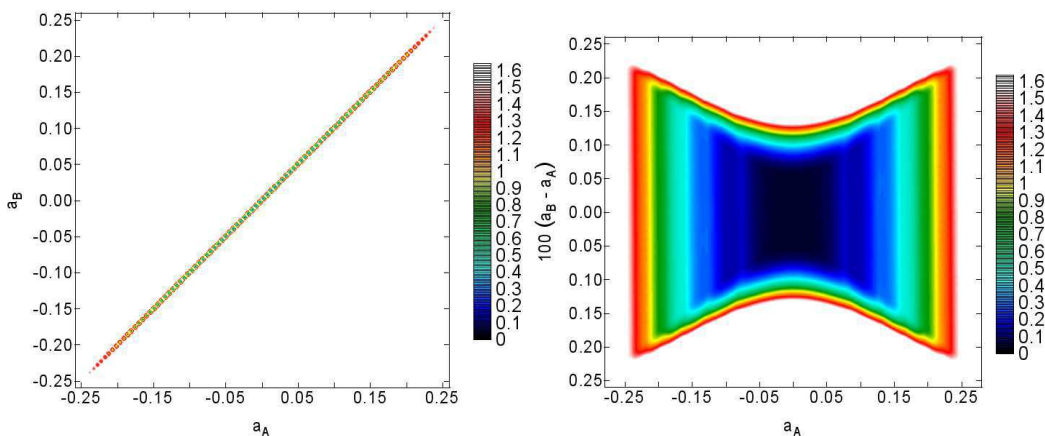


Figure 1: Contour plot of χ^2 for the Double Pulsar J0737-3039 as a function of a_A and a_B (left panel), and a function of $a_B - a_A$ and a_A (right panel). The value of χ^2 is minimized over m_A, m_B, b_A, b_B, k_A .

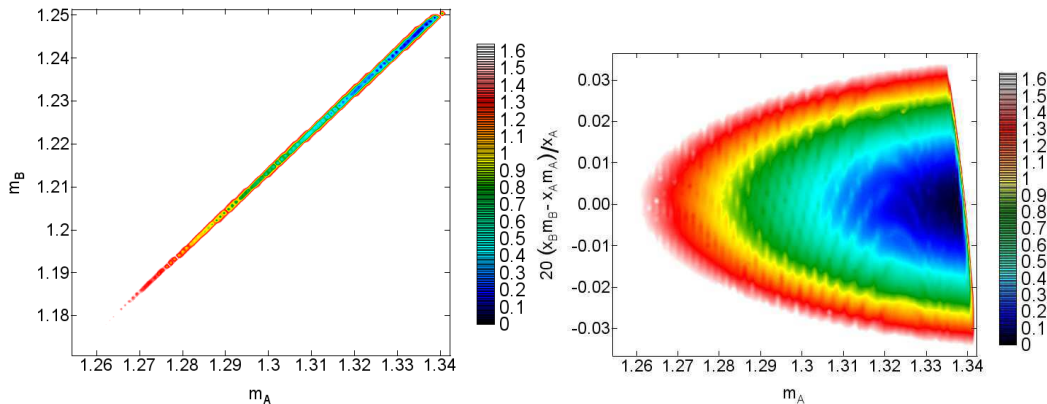


Figure 2: Contour plot of χ^2 for the Double Pulsar J0737-3039 in the $m_A - m_B$ plane (left panel). The right panel plots the same information using a variable that emphasizes the accuracy of the test of the prediction $R = m_A/m_B$. The value of χ^2 is minimized over a_A, a_B, b_A, b_B, k_A . Units on both axes are in solar masses.

Symbol	Meaning	Value
\dot{P}_b	Time derivative of orbital period	$-0.137(3)10^{-12}$
$\dot{\omega}$	Precession frequency of periastron	$1.755789(9)^\circ\text{yr}^{-1}$
γ	Relativistic timing parameter	2.070(2)
r	Range of Shapiro delay	$6.7(1.0)\mu\text{s}$
s	Shape of Shapiro delay	0.975(7)

Table 4: Post-Keplerian Parameters for PSR B1534+12. In the value reported for \dot{P}_b , the galactic and kinetic contributions have been subtracted.

do not depend on the particular form for the function $A(\phi)$ that defines which model is of interest, or on the details of the stellar equations of state. In particular we find that existing data impose strong and model-independent constraints on the relative size of the two scalar charges and masses.

These bounds can also be used to constrain particular models by computing in these models the masses and couplings as functions of the microscopic parameters. It is at this point that dependence on things like the stellar equation of state enters.

We applied these methods in particular to the double pulsar J0737-3039A/B, and found that $m_A = (1.31 \pm 0.03)m_\odot$, $m_B = (1.23 \pm 0.03)m_\odot$, $|a_{A,B}| < 0.25$, and $|a_B - a_A| < 0.0022$, with 95% confidence, for all choices of scalar-matter coupling function, and for all nuclear equations of state.

A similar analysis of the pulsar PSR B1534+12 yields $m_A = (1.1 \pm 0.2)m_\odot$, $m_B = (1.25 \pm 0.10)m_\odot$, $|a_{A,B}| < 0.44$, and $|a_B - a_A| < 0.0035$.

Acknowledgements

We wish to thank Marko Horbatsch for discussions and advice on numerical algorithms and

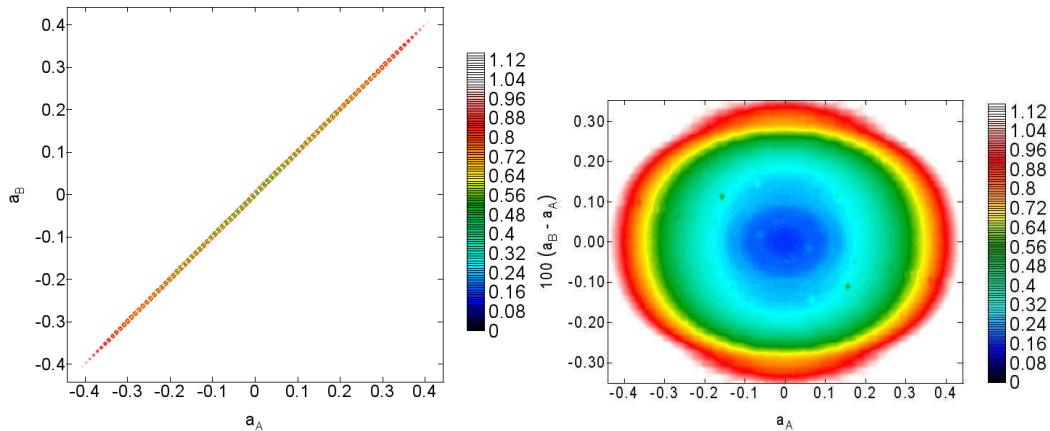


Figure 3: Contour plot of χ^2 for PSR B1534+12 in the $a_A - a_B$ plane (left panel), and with $a_A - a_B$ shown vs a_A (right panel). The value of χ^2 is minimized over m_A, m_B, b_A, b_B, k_A .

contour plots, Maxim Lyutikov for useful comments, and SHARCNET for computational resources. Our research is supported in part by funds from the Natural Sciences and Engineering Research Council (NSERC) of Canada. Research at the Perimeter Institute is supported in part by the Government of Canada through Industry Canada, and by the Province of Ontario through the Ministry of Research and Information (MRI).

References

- [1] D. R. Lorimer, Living Rev. Rel. **11** (2008) 8. [arXiv:0811.0762 [astro-ph]];
 G. S. Bisnovaty-Kogan, Phys. Usp. **49** (2006) 53. [arXiv:astro-ph/0611398];
 I. H. Stairs, Living Rev. Rel. **6** (2003) 5. [arXiv:astro-ph/0307536];
 I. H. Stairs, arXiv:astro-ph/0105090;
 V. M. Kaspi, arXiv:astro-ph/9912285;
 R. A. Hulse, Rev. Mod. Phys. **66** (1994) 699;
 J. H. Taylor, Rev. Mod. Phys. **66** (1994) 711;

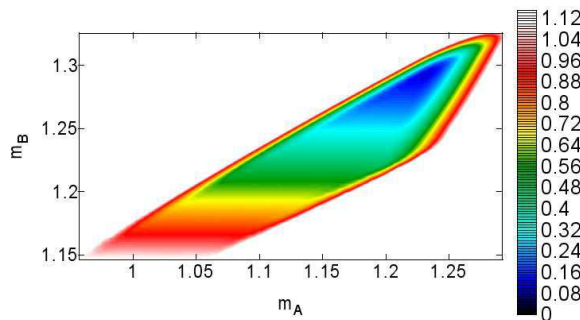


Figure 4: Contour plot of χ^2 for PSR B1534+12. The value of χ^2 is minimized over a_A, a_B, b_A, b_B, k_A . Units on both axes are in solar masses.

- J. H. Taylor and J. M. Weisberg, *Astrophys. J.* **345** (1989) 434;
 J. H. Taylor and J. M. Weisberg, *Astrophys. J.* **253** (1982) 908;
 R. A. Hulse and J. H. Taylor, *Astrophys. J.* **195** (1975) L51.
- [2] T. Damour, J. H. Taylor, *Phys. Rev.* **D45** (1992) 1840-1868;
 T. Damour and N. Deruelle, *Ann. Inst. Henri Poincaré* **44** (1986) 263-292;
 T. Damour and N. Deruelle, *Ann. Inst. Henri Poincaré* **43** (1985) 107-132;
 R. Blandford and S. A. Teukolsky, *Astrophys. J.* **205** (1976) 580.
- [3] I. H. Stairs, S. E. Thorsett, J. H. Taylor and A. Wolszczan, *Astrophys. J.* **581** (2002) 501.
 [arXiv:astro-ph/0208357];
 I. H. Stairs, D. J. Nice, S. E. Thorsett and J. H. Taylor, arXiv:astro-ph/9903289;
 I. H. Stairs *et al.*, arXiv:astro-ph/9712296;
 A. Wolszczan, *Nature* **350** (1991) 688.
- [4] I. H. Stairs, S. E. Thorsett and Z. Arzoumanian, *Phys. Rev. Lett.* **93** (2004) 141101
 [arXiv:astro-ph/0408457].
- [5] N. Wex and M. Kramer, arXiv:1001.4733 [gr-qc];
 M. Kramer and N. Wex, *Class. Quant. Grav.* **26** (2009) 073001;
 M. Kramer, I. H. Stairs, R. N. Manchester *et al.*, *Ann. Phys. (Leipzig)* **15** (2006) 34-42;
 M. Kramer, I. H. Stairs, R. N. Manchester *et al.*, *Science* **314** (2006) 97-102.
 [astro-ph/0609417];
 A. G. Lyne, *Chin. J. Astron. Astrophys.* **6** (2006) **Suppl. 2** 162-168;
 M. Kramer, D. R. Lorimer, A. G. Lyne *et al.*, [astro-ph/0503386];
 M. Kramer *et al.*, arXiv:astro-ph/0405179;
 A. G. Lyne *et al.*, *Science* **303** (2004) 1153. [arXiv:astro-ph/0401086].
- [6] R. P. Breton, V. M. Kaspi, M. Kramer, *et al.*, *Science* **321** (2008) 104-107.
 [arXiv:0807.2644 [astro-ph]].
- [7] C. H. Brans, [arXiv:gr-qc/0506063];
 V. Faraoni, *Cosmology in Scalar-Tensor Gravity*, Kluwer Academic Publishers 2004;
 Y. Fujii and K. Maeda, *The Scalar-Tensor Theory of Gravitation*, Cambridge University Press 2003;
 T. Chiba, T. Harada, and K. Nakao, *Prog. Theor. Phys. Suppl.* **128** (1997) 335;
 T. Damour and G. Esposito-Farèse, *Class. and Quant. Grav.* **9** (1992) 2093;
 T. Singh and L. N. Rai, *Gen. Rel. Grav.* **15** (1983) 875;
 K. Nordtvedt, *Astrophys. J.* **161** (1970) 1059;
 R. V. Wagoner, *Phys. Rev. D* **1** (1970) 3209;
 P. G. Bergmann, *Int. J. Theor. Phys.* **1** (1968) 25;
 R. H. Dicke, *Phys. Rev.* **125** (1962) 2163;
 C. Brans, *Phys. Rev.* **125** (1962) 2194;
 C. Brans and R. H. Dicke, *Phys. Rev.* **124** (1961) 925.

- [8] C. M. Will, arXiv:1008.0296 [gr-qc];
C. M. Will, Living Rev. Rel. **9** (2005) 3. [arXiv:gr-qc/0510072];
C. L. Lämmerzahl, in D. J. W. Giulini, C. Kiefer, and C. L. Lämmerzahl, eds., *Quantum Gravity: From Theory to Experimental Search*, vol. 631 of Lecture Notes in Physics, 367-394, (Springer, Berlin, Germany, 2003);
M. P. Haugan and C. Lammerzahl, Lect. Notes Phys. **562** (2001) 195. [arXiv:gr-qc/0103067];
C. M. Will. Theory and Experiment in Gravitational Physics, Revised Edition. Cambridge University Press, 1993.
- [9] K. Kainulainen and D. Sunhede, Phys. Rev. D **73** (2006) 083510. [arXiv:astro-ph/0412609];
A. Albrecht, C. P. Burgess, F. Ravndal and C. Skordis, Phys. Rev. D **65** (2002) 123507. [arXiv:astro-ph/0107573];
T. Damour and A. M. Polyakov, Gen. Rel. Grav. **26** (1994) 1171. [arXiv:gr-qc/9411069];
T. Damour and A. M. Polyakov, Nucl. Phys. B **423** (1994) 532. [arXiv:hep-th/9401069].
- [10] G. Esposito-Farese, AIP Conf. Proc. **736** (2004) 35-52. [gr-qc/0409081];
G. Esposito-Farese, [gr-qc/0402007];
T. Damour, G. Esposito-Farese, Phys. Rev. **D58** (1998) 042001. [gr-qc/9803031];
G. Esposito-Farese, arXiv:gr-qc/9612039;
T. Damour, G. Esposito-Farese, Phys. Rev. **D54** (1996) 1474-1491. [gr-qc/9602056].
- [11] T. Damour, [arXiv:0704.0749 [gr-qc]].
- [12] T. Damour and G. Esposito-Farèse, Phys. Rev. Lett. **70** (1993) 2220.
- [13] T. Damour, in 300 Years of Gravitation, ed. S. W. Hawking and W. Israel, Cambridge University Press 1987, pp.128-198.
- [14] H. Goldstein, C. P. Poole, J. L. Safko. Classical Mechanics, 3rd Edition. Addison Wesley, 2001. Section 10.8.
- [15] M. W. Horbatsch, C. P. Burgess, JCAP (2011) (in press). [arXiv:1006.4411 [gr-qc]].
- [16] T. Damour and J. H. Taylor, Astrophys. J. **366** (1991) 501.